3-11-2010

Structure-Property Relationship in Ionomer Membranes

Ahmet Kusoglu
University of Delaware

Anette M. Karlsson
Cleveland State University, a.karlsson@csuohio.edu

Michael H. Santare
University of Delaware

Publisher's Statement

NOTICE: this is the author's version of a work that was accepted for publication in Polymer. Changes resulting from the publishing process, such as peer review, editing, corrections, structural formatting, and other quality control mechanisms may not be reflected in this document. Changes may have been made to this work since it was submitted for publication. A definitive version was subsequently published in Polymer, 51, 6, (03-11-2010);

Original Citation

Kusoglu, A., Karlsson, A. M., and Santare, M. H., 2010, "Structure-Property Relationship in Ionomer Membranes," Polymer, 51(6) pp. 1457-1464.

Structure-property relationship in ionomer membranes

Ahmet Kusoglu, Anette M. Karlsson*, Michael H. Santare

Department of Mechanical Engineering, University of Delaware, Newark, DE 19716, USA

1. Introduction

Perfluorosulfonic acid (PFSA) membranes are sulfonated ionomers with a hydrophobic poly-tetrafluoroethylene (PTFE) backbone [1]. PFSA membranes have good ionic conductivity and thermo-mechanical stability and are therefore commonly used as electrolytes in electrochemical devices such as proton exchange membrane (PEM) fuel cells [1–5].

The hydrophobic PTFE-like backbone of the ionomer membrane maintains the structural integrity and the ionic (sulfonic acid) groups can attach to water molecules. Thus, in the presence of water, hydrophilic water-filled ionic domains, or *pores*, are formed enabling ion conductivity [2,6–8]. Therefore, the mechanical properties (e.g. Young's modulus) and the physical properties (e.g. conductivity) of the PFSA membrane are both directly linked to the nanostructure (e.g. pore shape and size). These properties can be engineered to meet the conductivity levels required for an efficient cell operation while maintaining the necessary structural stability [2–5].

Swollen PFSA ionomers have a phase-separated morphology, where the water and ions form hydrophilic domains separated from the hydrophobic polymer matrix [6,8–18]. Pioneering work of Gierke, Hsu and co-workers [8,11] introduced the *cluster-network model*, i.e. spherical water-filled ionic clusters connected with cylindrical water-filled channels. The water-filled domains are dispersed in the polymer matrix with sulfonic acid (SO_3^-) ionic groups located along the interface between the water and polymer. Since then, several other nanostructural descriptions have been proposed, including the studies by Dreyfus et al. [16] on the distribution of clusters in the polymer matrix; by Gebel [6,17] on the transition from spherical-interconnected clusters to rod-like structure at high degree of swelling; by Haubold et al. [18] suggesting a sandwich-like model for two-phase morphology; and recently by Schmidt-Rohr and Chen [7] who proposed a cylindrical water-filled channel model. Other possible interpretations of the two-phase nanostructure are discussed in Gruger et al. [19], Weber and Newman [20], Kim et al. [21] and Termonia [22]. Furthermore, rod-like polymeric aggregates with water pools residing among them have been suggested for highly-swollen PFSA ionomers [6,15,23,24]. An extensive discussion and comparison of the nanostructures can be found in refs. [1,7,25].

However, a full description of the relationship between the nanostructure and mechanical properties in swollen PFSA membranes is yet to be established. In our previous work, we proposed mechanics-based models to determine Young's modulus of PFSA membranes in humid air [26], and to determine water content in PFSA as a function of humidity [27]. In this work, we will investigate the influence of temperature and water content on the structure-property relationship by extending the previous work on Young's modulus [26] to high water contents and, with the help of our previously-developed sorption model [27], to sub-zero temperatures. Specifically, we aim to discuss, from a mechanics perspective, the evolution of the nanostructure-property

* Corresponding author. Tel.: +1 302 831 6437.
E-mail address: karlsson@udel.edu (A.M. Karlsson).

relationships in PFSA membranes during water uptake. We will base the discussion on our published [28,29] and unpublished experimental data, and other researchers' published work on morphology and water content of these membranes [6,7,19,20,22].

2. Theory and model

2.1. Evolution of nanostructure with water uptake

In the presence of an external water source, water molecules diffuse into the PFSA membrane by attaching to the hydrophilic ionic sulfonic acid (SO_3^-) groups, resulting in growth of the water-filled ionic domains that are surrounded by the hydrophobic backbone [2,6,8,18–20,30,31]. This corresponds to the macroscopic swelling in the membranes. The number of water molecules attached to each ionic (SO_3^-) group is designated λ, and is related to the water uptake in the membrane:

$$\lambda = \frac{[H_2O]}{[SO_3^-]} = \frac{W_p^{swollen} - W_p^{dry}}{W_p^{dry}} = \frac{\phi_w}{1-\phi_w}\frac{\overline{V}_w}{\overline{V}_p}, \quad (1)$$

where W_p is the weight of the polymer membrane, $\phi_w (= 1 - \phi_p)$ is the water volume fraction, and $\overline{V}_w$ and $\overline{V}_p$ are the molar volume of water and dry polymer, respectively. $\overline{V}_p$ is related to the *equivalent weight* (EW) and density, ρ_p, of the membrane through the equation, $\overline{V}_p = EW/\rho_p$.

In our previous work [26] we proposed a mechanics-based model to determine Young's modulus of *vapor-equilibrated* PFSA membranes (swollen in humid air) based on the morphological descriptions of this polymer at moderate water content as described in the literature [6,8,11,16,20,21]. In that work, we introduced the *Sphere-Channel Representative Volume Element (RVE)* comprised of a cubic volume element of length, d, which contains a single spherical *cluster* of diameter, d_s, and four cylindrical channels of diameter, d_{ch}, lying on the diagonals of the cube (Fig. 1A) [26]. The idealized geometry is chosen to be isotropic, corresponding to the experimental observation of in-plane isotropy [29].

Since both Young's modulus and conductivity change with changes in the morphology of the water-swollen PFSA membranes, the geometric features of the water domains used to model Young's modulus should be related to those used to characterize conductivity. The conductivity of PFSA membranes, κ_c, increases with water uptake (or swelling) [3,5,6,8,32–39] and is assumed to be related to the water volume fraction according the equation, $\kappa_c \propto \phi_w^s$ where the exponent, s, is empirically determined to be between 1.0 and 1.95 [8,33,35,36]. This relationship can be attributed to the growth of water-swollen ionic domains: both the interconnecting channels and spheres expand during water sorption [6,10,21,35,39–41]. The exact relationship between conductivity and water content is complicated and controlled by various transport mechanisms as well as the properties of the channel-like porous structure [8,34,35,39,42–45]. However, in order to incorporate the concept of expanding water-channels into our model, we have simply introduced a geometric *channel parameter*, $k = d_{ch}/d_s$ (Fig. 1A) [26]. In our previous work we showed that when k is set to the water volume fraction (i.e. $k = d_{ch}/d_s = \phi_w$) the model predictions for Young's modulus of PFSA membranes match the experimental data quite well [26]. Proportionally of k to ϕ_w suggests that the size of the interconnecting channels increase with water uptake, which might be associated with the increase in conductivity. Thus, using water-filled interconnecting channels in our model for Young's modulus is consistent with the conductivity behavior. The temperature-dependence of the conductivity is well documented in the literature [3,5,34,36,38,46–48]. However, we will here, for simplicity, assume that the pore shape and connectivity in the nanostructure is not influenced by the temperature, since there is evidence to support this elsewhere [36,49]. The temperature dependence can easily be incorporated in an extension of this work.

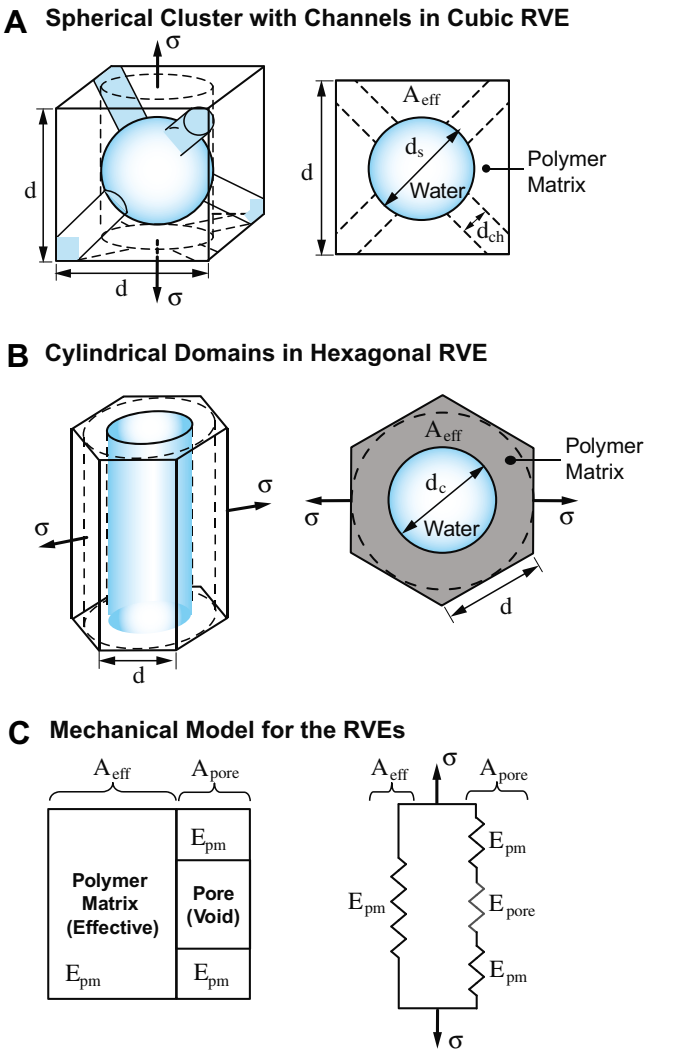

Fig. 1. Representative volume elements (RVEs) used in the mechanics model for water domains in the form of (A) spherical clusters with interconnecting cylindrical channels, and (B) cylinders. (C) Mechanical analogy for the elastic deformation of the RVEs (adapted from ref. [26]).

2.2. Model for Young's modulus of PFSA in water vapor

We previously developed a mechanics-based modeling framework to characterize the distribution of the load-bearing hydrophobic regions and the water absorbing hydrophilic domains in the assumed RVE [26]. This model was shown to capture the elastic behavior of vapor-equilibrated PFSA membranes with low to moderate water volume fractions ($0 < \phi_w < 0.25$ or $0 < \lambda < 15$). We will here extend the model to consider alternate nanostructures and higher water contents. We assume that in tension, the mechanical force is carried by the solid phase of the ionomer (i.e. the *polymer matrix*) surrounding the cluster and channels, while the water and ions form the *pores* that act as a non-load-bearing void. Consequently, the ratio of (effective) Young's modulus of the swollen ionomer, E_{eff}, to that of the PTFE-like polymer matrix, E_{pm}, can be associated with the fraction of the load-bearing *effective area* of the polymer matrix, $A_{eff} (= A_{pm})$, to the total area of the RVE, A:

$$\frac{E_{\text{eff}}}{E_{\text{pm}}} = \frac{A_{\text{eff}}}{A} = \frac{A_{\text{pm}}}{A} = 1 - \frac{A_{\text{pore}}}{A} = g\left(\phi_{\text{pore}}\right) \tag{2}$$

In Eq. (2), the function g represents the conversion of the volume fraction of the pores (water and ions), $\phi_{\text{pore}} = \phi_w + \phi_{\text{ion}}$, to the pore area fraction, A_{pore}/A, based on the projection of the RVE geometry onto the surface perpendicular to the loading direction (Fig. 1A). The derivation of $g(\phi_{\text{pore}})$ is outlined in our previous work [26]. Thus, the water content is assumed to affect only the pore size and shape, and determines the effective load-carrying area. The temperature dependence of the PFSA is incorporated via a temperature-dependent Young's modulus of the polymer matrix, E_{pm}. Experimental investigations suggest that Young's modulus of PFSA membrane changes with temperature even at very low water contents [26,29,50,51]. Based on the geometric assumptions in our model, the diameter of the spherical pores divided by the RVE length increases with pore fraction according to $d_{\text{pore}}/d \cong d_s/d = \phi_{\text{pore}}^{0.30}$ [26].

The polymer matrix fraction, $\phi_{\text{pm}} = 1 - \phi_{\text{pore}}$, can be used as an alternative to the pore volume fraction, ϕ_{pore}, in Eq. (2). In this case, the function on the right-hand side of Eq. (2) can be written in the form of a power-law relationship:

$$\frac{E_{\text{eff}}}{E_{\text{pm}}} = \phi_{\text{pm}}^{\text{m}} = \left(1 - \phi_{\text{pore}}\right)^{\text{m}} \tag{3}$$

where m is the *scaling exponent* characterizing the structure-property relationship and is found to be m = 3.62 for the sphere-channel model (see ref. [26] for details).

Since the ionic groups cluster even in a dry membrane [6,11,52,53] the model reduces to a *spherical cluster in a cubic RVE* without channels when the membrane is completely dry ($k = 0 \approx \phi_w$). Thus, for this case, $\phi_{\text{pore}} = \phi_{\text{ion}}$. If we assume that the interconnecting channels never form and all the pores remains spherical, then the relative scale of the spherical pores is slightly different, $d_{\text{pore}}/d = \phi_{\text{pore}}^{0.33}$, and Eq. (2) simplifies to

$$\frac{E_{\text{eff}}}{E_{\text{pm}}} = 1 - C_g \phi_{\text{pore}}^{2/3} \tag{4}$$

where the geometrical factor is $C_g = (9\pi/16)^{1/3} = 1.208$ [26]. For spherical water domains, the scaling exponent in Eq. (3) becomes m = 1.9. Thus, we see that the scaling exponent is a function of geometry and structural connectivity.

When the membrane is dry, $\phi_w = 0$, and consequently $\phi_{\text{pore}} = \phi_{\text{ion}}^{\text{dry}}$, the pores correspond to the clustered ionic sulfonic acid groups. In this case, Eq. (3) provides a relationship between Young's modulus of the polymer matrix (excluding the ionic clusters), E_{pm}, and Young's modulus of the dry PFSA membrane (including the ionic clusters), E_{dry}, which is a function of temperature only. Therefore, the effective Young's modulus can also be rewritten in terms of E_{dry}:

$$\frac{E_{\text{pm}}}{E_{\text{dry}}} = \frac{\phi_{\text{pm}}^{\text{m}}}{\left(1 - \phi_{\text{ion}}^{\text{dry}}\right)^{m}} \text{ and } \phi_{\text{ion}}^{\text{dry}} = \frac{\overline{V}_{SO_3}}{\overline{V}_{\text{p}}} \approx \frac{40.94}{EW/\rho_p}. \tag{5}$$

Based on this model, Young's modulus of dry PFSA of 1100 EW at room temperature is predicted to be 254 MPa [26]. This value is similar to those reported for an almost dry PFSA (measured at RH < 5%) in a number of studies: 250–270 MPa depending on strain-rate in ref. [54]; 225 MPa [50,55,56]; 225–250 MPa [56].

2.3. Model for Young's modulus of PFSA in liquid water

It is well documented that *liquid water-equilibrated* PFSA membranes (swollen in liquid water) have different physical properties than those swollen in water vapor (humid air) [6,10,19,28,35,39,42,43,47,57]. This difference may be attributed to significantly higher water contents $\lambda = 21 - 24 (\phi_w = 0.40 - 0.45)$ in liquid water with relatively weak temperature dependence [19,39,42,43,47]. Pretreatment of the membrane can also affect the maximum water uptake in liquid water [42,47]. Since the experimental data used in this work is obtained from the testing of preboiled PFSA membranes [29], for consistency we will only use the sorption data obtained for the membranes subjected to the same pretreatment.

For water volume fractions higher than 0.45, it is difficult to obtain a physically reasonable geometry and packing of the spherical cluster-channel model proposed in the previous section. Interestingly, recent work by Schmidt-Rohr and Chen [7] suggested an alternative model for the nanostructure of swollen PFSA membranes: parallel water-filled cylindrical nano-channels distributed in the polymer backbone with ionic groups along the interface between the water and polymer. This model has been shown to capture the experimental scattering curves better than spherical cluster-channel models at high water contents [7]. Also, the nanostructure of a highly-swollen PFSA membrane has been shown to be comprised of repeating PTFE units, similar to the helical molecular structure of PTFE, surrounding the water domains [14,19,58]. In light of these results, we propose an alternative model for highly-swollen PFSA membrane: *cylindrical water domains* surrounded by polymer backbone in hexagonal RVEs (Fig. 1B). For this geometry, the relative diameter of the cylindrical pores varies with pore fraction through the relation $d_{\text{pore}}/d = d_c/d = \phi_{\text{pore}}^{0.50}$. This results in an in-plane, transversely isotropic behavior of the membrane.

Using the same geometric derivation described previously for the spherical water domains, the effective modulus for the cylindrical RVE becomes

$$\frac{E_{\text{eff}}}{E_{\text{pm}}} = \frac{A_{\text{eff}}}{A} = 1 - \frac{2}{3}\frac{d_c}{d} = 1 - C_g \phi_{\text{pore}}^{1/2} = \phi_{\text{pm}}^{\text{m}} \tag{6}$$

where the geometrical factor is $C_g = 1.212$[1], and the scaling exponent is m = 2.41.

3. Results and discussion

3.1. Young's modulus of vapor-equilibrated PFSA membrane

Model predictions for Young's modulus as a function of water volume fraction for PFSA membrane of 1100 g/mol EW at 25 °C are depicted in Fig. 2. The results shown are for the spherical domains with channels and without channels. These are compared to the experimental data for vapor-equilibrated PFSA membrane obtained at various water volume fractions between 0.08 and 0.25 [29]. Young's modulus of the polymer matrix, E_{pm} and of the dry membrane, E_{dry}, are included for comparison. The figure suggests that including expanding interconnecting channels in the RVE, in addition to the spheres, gives the best agreement with the experimental data in this range of water content.

3.2. Young's modulus of liquid-equilibrated PFSA membrane

Model predictions and experimental data for Young's modulus for 1100 EW PFSA membrane equlibrated in liquid water are depicted in Fig. 3 at selected temperatues [28]. The standard

[1] Structural factor is determined from the geometry of cylinder and hexagon as: $C_g = 3(12\sqrt{3}/2\pi)^2/2$.

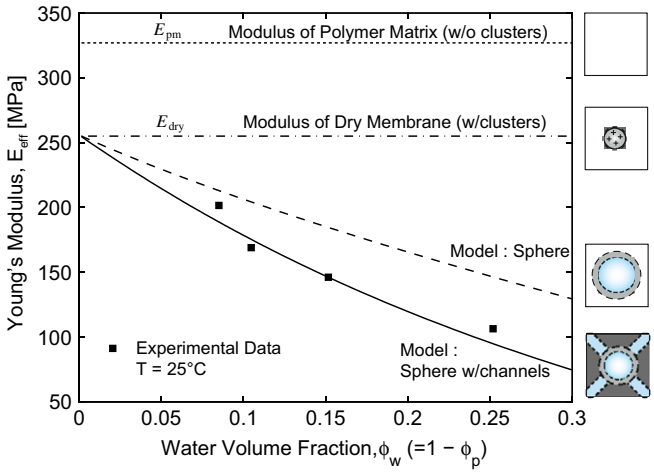

Fig. 2. Young's modulus of PFSA membrane as a function of water volume fraction at 25 °C: model predictions (solid lines) vs. experimental data for vapor-equilibrated membrane (markers) [29].

deviation of the measured water volume fraction of the membrane is $\phi_w = 0.41 \pm 0.02 (\lambda = 22 \pm 2)$. Therefore, the model predictions for Young's modulus, Eq. (6), are plotted in Fig. 3 within these limits (shaded area). For comparison, the predictions of Eq. (3) based on sphere-channel and sphere only water domains ($m = 3.6$ and 1.9, respectively) are included in Fig. 3 for the water content of $\lambda = 22$. As can be seen from Fig. 3, the calculated Young's modulus based on cylindrical water domains gives the best agreement with the measured values, suggesting that the best structural description for the liquid-equilibrated PFSA membrane is cylindrical water-filled pores. Also, the ratio of the water-filled pore diameter to the thickness of the backbone separating these pores is found to be 4.5, which is in agreement with the values reported in the literature for swollen PFSA membranes [7,8,14].

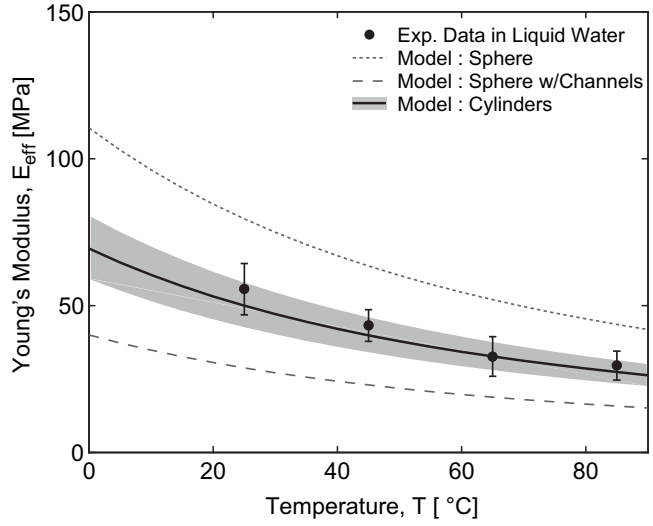

Fig. 3. Predictions of the mechanics model for Young's modulus of PFSA membrane equilibrated in liquid water as a function of temperature compared to the experimental data [28]. Three models are considered: water domains in the form of (i) spheres, (ii) spheres with expanding cylindrical channels, and (iii) cylinders. The model predictions for cylindrical water domains are shown as a band where the upper and lower limit corresponds to the standard deviation in the measured water content, $\phi_w = 0.42 \pm 0.02$. The other two models are plotted for $\phi_w = 0.42$.

3.3. Structural transition during water uptake

Given the good agreement between the predictions of the selected RVEs and the experimental data, we propose that there is a structural transformation in PFSA ionomers associated with changing water content. Eq. (3) can be used to determine the effective Young's modulus for all the selected geometries by changing the scaling exponent, m, to the values 1.9, 3.62 and 2.41 for the spherical, sphere-channel and cylindrical water domains, respectively. The model predictions for the normalized effective Young's modulus (E_{eff}/E_{pm}) based on all three geometries are plotted in Fig. 4 together with the experimental data [28,29]. Note that, within the context of the model, temperature affects only the polymer matrix modulus, E_{pm} (see Eq. (8)). Thus, by normalizing Young's modulus with E_{pm}, the temperature-dependence is not shown in Fig. 4, and only the influence of water content on the elastic response is displayed explicitly.

Recall that the dry membrane has clustered SO_3^- ions in spherical form and therefore has a lower Young's modulus (E_{dry}) than the polymer matrix alone (which actually is a hypothetical material, E_{pm}). This is represented by the shaded region, ϕ_{ion}, in Fig. 4, corresponding to a theoretical transition range. For low pore fractions, $\phi_{pore} < 0.1$, the difference between the model predictions for spherical and sphere-channel geometries is small and therefore difficult to distinguish experimentally (Fig. 4). However, based on the experimental evidence of the existence of spherical ionic clusters [6,11,52,53], we believe that the porous domains are most likely to be spherical, with a small amount of water attached to the ionic groups. When the water volume fraction (and consequently the pore fraction) increases, the sphere-channel model appears to become a more accurate description of the nanostructure. Since the critical water fraction for the initiation of ion conduction (*percolation*) has been shown to be less than $\phi_{pore} = 0.10$ for PFSA membranes [8,33,35], this may be associated with the threshold for the formation of interconnecting channels between spherical domains. From low to moderate water contents ($0.1 < \phi_{pore} < 0.3; 2 < \lambda < 15$), the model with spheres with expanding channels demonstrates good agreement with the

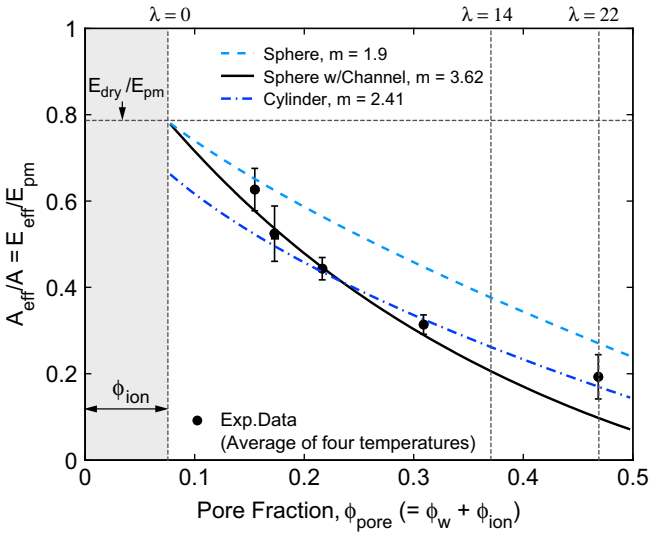

Fig. 4. Predictions of normalized Young's modulus of PFSA membrane as a function of pore volume fraction compared with the experimental data from Tang et al. [29] (vapor-equilibrated) and Kusoglu et al. [28] (liquid-equilibrated). Three models are considered: water domains in the form of (i) spheres, (ii) spheres with expanding interconnecting channels, and (iii) cylinders only.

experimental data. However, for higher water contents ($0.36 < \phi_{pore} < 0.50; 15 < \lambda < 22$), the cylindrical model gives a better representation of the measured Young's moduli (Fig. 4). Thus, when the water is confined in cylindrical domains instead of a sphere-channel network, the ionomer gets stiffer relative to the sphere-channel approximation. In the model, this is due to the fact that more of the hydrophobic polymer matrix becomes load-bearing in the cylindrical configuration as compared to the sphere-channel geometry.

$$E_{pm}(T<0) \Rightarrow \left\{ \begin{array}{ll} MODEL & \Rightarrow RH \rightarrow \quad \phi_w \\ ELASTIC & \\ MODEL & \Rightarrow \phi_w \rightarrow \quad E_{eff} \end{array} \right\} \Rightarrow E_{eff}(RH, T<0) \rightleftarrows E^*(RH, T<0) \leftarrow \tag{7}$$

These results reveal some interesting features regarding the vapor-to-liquid transition of PFSA membranes: the change in the scaling exponent, m, (due to a possible change in the morphology, porous structure etc.) is consistent, at least qualitatively, with the findings of conductivity and sorption behavior of PFSA membranes in this regime ($15 < \lambda < 22$) [20,35]. The conductivity of the PFSA membranes increases during water uptake [6,8,32,34–39,59], probably due to larger hydrophilic domains [2,6–8,19,35,39,45,59]. In a similar manner, increasing water leads to a decrease in the fraction of load-bearing hydrophobic domains and consequently reduces Young's modulus.

In this work, we use the (nano-) structure to predict the mechanical properties. The surface energy, as well as the size and the shape of the domains, are all related through the electro-static interaction energy, which can be used to study the structure and clustering [8,60,61]. This could, for example, explain the transition in the structure from spheres to cylinders. However, there are many challenges involved with developing a complete model starting with surface and interaction energy to predict mechanical properties, due to the high number of independent parameters characterizing the electro-chemical interactions and therefore such a model is beyond the scope of this work.

3.4. Extension of model to sub-zero temperatures

The mechanics-based model developed in this paper is shown to capture the experimentally observed elastic behavior of PFSA membrane above room temperatures. We will now show how we can employ these models to predict Young's modulus at temperatures below 0 °C. One main challenge to this analysis is the lack of information in the literature on the relationship between the membrane's water content, λ, and humidity at low temperatures. To overcome this challenge, we will use the mechanics-based model we developed previously for the sorption behavior of PFSA membrane [27]. This model predicts the water fraction, ϕ_w, (or water content, λ) as a function of relative humidity, RH, for a given temperature-dependent polymer matrix modulus, $E_{pm}(T)$ (see Appendix). Thus, by combining (i) the mechanics model (we presented here that predicts the effective Young's modulus, E_{eff}, as a function of water fraction, ϕ_w) and (ii) the sorption model [27] (that predicts water fraction, ϕ_w, as a function of relative humidity, RH), we can predict Young's modulus at below-freezing temperatures. We note that Young's modulus of the polymer matrix, $E_{pm}(T)$, is a temperature-dependent parameter in both models. Thus, once we know $E_{pm}(T)$ at sub-zero temperatures, i.e. $T < 0$, we can find both the water fraction and the effective modulus as a function of relative humidity. In order to determine $E_{pm}(T)$ for $T < 0$, we will use a limited set of experimental Young's modulus data[2] we have developed for temperatures below zero, $E^*(RH, T < 0)$, to validate the Young's modulus predicted by the model $E_{eff}(RH, T < 0)$. The experimental data is limited due to the difficulties associated with controlling and measuring the relative humidity at low temperatures. In summary, the general approach taken in the following is

We first need to explore the applicability of the models, i.e. the assumption that that the water domains in the membrane remain in a liquid phase and therefore act as voids in tension at sub-zero temperatures. The water in PFSA membrane is classified as *non-freezable* if it is strongly bound to the backbone and *freezable* if it is free to move and expected to crystallize upon cooling. The number of non-freezable water molecules in a PFSA membrane is reported to correspond to $\lambda \sim 6$–7, independent of the initial water content of the membrane at room temperature [36,38,39,46,62], with the remaining water, if any, being freezable. Thus, the higher the membrane's initial water content at above-zero temperatures, the higher the amount of freezable water the membrane will have upon cooling [36,38,46]. The freezing temperature of water in a highly hydrated PFSA membrane ($\lambda \sim 18$–24) is around −2 to −5 °C, thus close to that of pure water [36,46,48,63]. However, the freezing temperature gradually decreases with decreasing water content and eventually reaches −40 to −50 °C for low water contents ($\lambda < 4$–6) [36]. This is attributed to the depression of the freezing point with decreasing water content in PFSA membranes [36,38,39,46,48,62]. Observations also indicate that the conductivity of PFSA membrane continues to decrease when the temperature decreases below 0 °C [36,46,48] and almost vanishes at around −45 °C [36,38]. Based on these observations, we will assume the water in the membrane to be liquid, without any ice formation, for the temperature-water content range of interest (T>−40 °C, $\lambda < 7$) [36].

The polymer matrix modulus, E_{pm}, calculated from the simultaneous solution of the two models is found to increase with decreasing temperatures (Fig. 5A) obeying an Arhenius type relationship

$$\frac{E_{pm}(T)}{E_{pm}(298)} = \exp\left[\frac{E_{ae,pm}}{R}\left(\frac{1}{T} - \frac{1}{298}\right)\right], \tag{8}$$

where $E_{ae,pm}$ is the activation energy, R is the universal gas constant and T is the absolute temperature [K] with 298 K being the reference temperature. The activation energy is found to be 10.66 kJ/mol, very close to that reported for PTFE [64]. This is not surprising, since our results are in agreement with the experimentally observed trends for the temperature-driven decrease in Young's modulus of PFSA membrane [9,62,63] and of PTFE [65] at sub-zero temperatures.

Using the calculated E_{pm} at sub-zero temperatures, we can first determine the approximate water volume fraction for a given humidity at temperatures below 0 °C and then use this value in the micro-mechanics model presented in section 2, to calculate the effective modulus for the sphere-channel water domain model. The

[2] Experimental data for Young's modulus at freezing temperatures is obtained as part of our on-going research on the tensile testing of PFSA membranes at temperatures below zero.

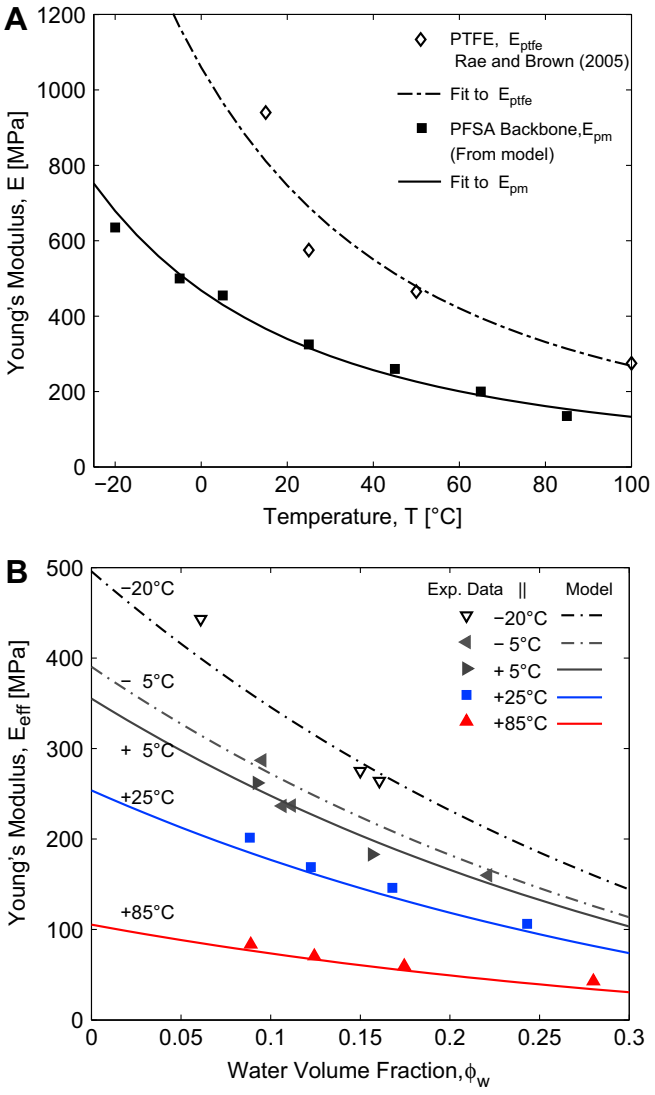

Fig. 5. The results of the solutions of the models for (A) polymer matrix modulus, E_{pm}, as a function of temperature, and (B) variation of Young's modulus of PFSA membrane, E_{eff}, with water volume fraction at subfreezing temperatures shown together with the preliminary experimental data.

proposed model predictions for Young's modulus at sub-zero temperatures are in good agreement with the preliminary experimental data (Fig. 5B). We note that when the sorption model adopted from our previous work [27] is used to convert humidities to water volume fractions instead of formulations from the literature (e.g. refs. [34,66] and [26]), the model predictions still agree well with experimental data through a wide range of temperatures (from −20 °C to 85 °C).

4. Scaling behavior: analogy to other porous structures

Up to now, we have shown how the geometry of the porous water domains affects Young's modulus of PFSA membranes; in particular that the structure-property relationship of swollen PFSA membranes can be characterized by the scaling exponent, *m*, which depends solely on the shape of the water domains in the nanostructure (see Eqs. (5)–(6) and Fig. 4). We will now discuss the structure-property relationship of other porous materials and compare their scaling exponents with those found for PFSA membranes in the present work.

4.1. Foam structures

The mechanical behavior of porous cellular structures (or foams) is commonly characterized by relating the elastic properties to the density, or volume fraction of the *solid phase*, ϕ_{sp}, and structural features of the solid (e.g. topology, interconnectivity and pore shapes) [67]. The upper and lower limits for the scaling behavior of the modulus are characterized by the scaling exponent m=1 (in Eq. (3)) for *closed-cell* structures, where the solid faces contribute to the mechanical response, and m =~~2~~ for *open-cell* structures, where only the edges are solid and contribute to the mechanical response [67–69]. If the effective modulus, as a function of the fraction of the solid phase of the PFSA, is plotted in a logarithmic scale, the scaling exponents represent the slope (Fig. 6). The dominant mode of deformation (e.g. bending or axial stretching) is also another important factor for the modulus-fraction scaling behavior [67,68].

For the purposes of calculating the tensile modulus, PFSA membrane can be considered a porous network even though the pores are filled with water. For example, Termonia [22] suggested that with increasing water fraction the plate-like backbone in the nanostructure of PFSA membrane stretches into narrow ribbons connected at entanglement points. This molecular level description can be interpreted as a transition from closed-cell to open-cell behavior. We note that predictions for the open-cell foam (m =~~2~~ in Fig. 6) demonstrate a trend similar to our model predictions for spherical water domains (for which m =~~1.9~~). However, the scaling exponent for swollen PFSA membrane (m∼3.6) is much higher than those given for foams (m∼1–2) (Fig. 6). This deviation can be attributed to the fact that, in the sphere-channel model, some of the solid regions are ineffective due to the connectivity of the pores and therefore do not contribute to the mechanical stiffness.

4.2. Aerogels

Aerogels are highly porous materials obtained by removing the liquid part of the wet gel (Alcogel) without altering the solid structure. The gel network has a self-similar dendritic nanostructure consisting of pores of varying size (nano to micro-meter

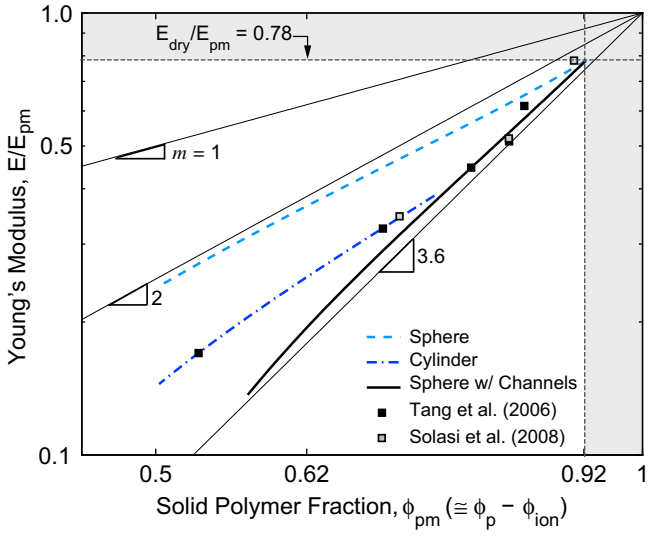

Fig. 6. Scaling of Young's modulus with solid (hydrophobic) polymer phase fraction as determined from our model for selected geometries (lines) shown together with the experimental data (markers) for PFSA membrane from Tang et al. [29] and Solasi et al. [55] (vapor-equilibrated), and Kusoglu et al. [28] (liquid-equilibrated). (The slopes $m = 1$, 2 and 3.6 represent the closed-cell foams, open-cell foams, and aerogels, respectively.).

in size) [70] interconnected through micro-particles. The structure gets stiffer with increasing connectivity, e.g. the diameter of the solid bridges connecting the particles [71,72]. The mechanical properties scale with the density, but it is the connectivity that determines the scaling behavior [72–75]. Thus, the scaling exponent is attributed mainly to the connectivity between these particles (or pores) [74,75], which might change with the processing (gelation, aging and shrinkage), but not with the structural features inside the clusters, e.g. fractal dimension, spectral dimension, tortuosity [73,75,76]. Thus, from a mechanics perspective, under an applied tensile load, both aerogels and ionomers can be considered structurally as interconnected solids surrounding the voids with zero tensile modulus.[3]

Interestingly, the scaling exponent, m, for PFSA is very similar to those reported for aerogels made from silica gels: $3.2 \leq m \leq 3.7$ (depending on the processing) [74–77] and a little lower than colloid gels, for which $m = 4$ [78]. It has been shown that the cellular solid analogy does not capture the scaling behavior of aerogels, since not all solid areas contribute to the load transfer [72]. Thus, even though the PFSA ionomers and aerogels are very different in nature, they have a similar scaling behavior for Young's modulus, suggesting that their geometric nanostructural features could be correlated and should be investigated further. These observations are consistent with our hypothesis that the structure-property relationship of ionomers and aerogels can be similarly studied using only the geometric features of their nanostructure.

5. Concluding remarks

The structure-property relationship in PFSA membranes exposed to humidity and temperature changes is investigated using a mechanics-based approach for a number of possible representative geometries. Our results suggest that Young's modulus is controlled by the morphology and water content of the membrane. This finding, when considered together with the well documented water-dependence of the conductivity, indicates a correlation between the physical properties (e.g. conductivity) and mechanical properties (e.g. Young's modulus). Unfortunately, environmental conditions that improve the conductivity might be detrimental to the mechanical properties. For example, larger water uptake at a given temperature leads to an increase in the fraction of hydrophilic pore-like water-swollen domains, and consequently the fraction of hydrophobic polymer backbone decreases. The first effect may be associated with enhanced conductivity, whereas the latter is shown to lead to a reduction in Young's modulus. The effect of temperature on the modulus of the membrane can be associated with the temperature-dependent modulus of the polymer backbone.

A comparison between experimentally measured Young's modulus and the predictions of our proposed model, for selected representative geometries, reveals a possible nanostructural transition during sorption. At low water contents (λ<2–3) the nanostructure of the membrane can be characterized by spherical, hydrophilic domains distributed in the hydrophobic polymer matrix. With increasing water uptake, channels connecting these spheres form. These channels expand, along with the spheres, with increasing water content, λ, leading to an interconnected porous structure. However, at higher water contents between saturation in vapor and equilibrium in liquid water, i.e. (15<λ<25), a nanostructure consisting of cylindrical water-filled domains surrounded by the PTFE backbone provides a better fit to the measured properties.

The morphologies discussed here for the PFSA ionomers have been suggested based on scattering experiments [6,15,17–19,21,37] and theoretical models [7,20,22,45] in the literature. This work combines these findings with our mechanics-based nanostructural models, suggesting a structural transition with water uptake based on the concept that the mechanical properties are dominated by the morphological changes. Moreover, comparison of the scaling behavior for the PFSA membrane (based on our model and experimental data) and that for other porous materials suggest that the connectivity of the structural porous network for the swollen ionomer membranes is closer to that for an aerogel than it is for open- or closed-foams. We believe the findings presented here provide a clear indication of the structure-property relationships in ionomer membranes.

Acknowledgements

Funding for portions of this work was provided by University of Delaware, W.L. Gore and Associates, Inc.

Appendix

Here we review the sorption model for PFSA membranes proposed by Kusoglu et al. [27]. In swelling equilibrium, the confining pressure applied by the polymer matrix on the water domains is balanced by osmotic swelling pressure of the water domains (i.e. the tendency of external moisture to diffuse into the membrane and increase the swelling). Therefore, if the relationship between the swelling pressure and the water volume fraction is known, the sorption behavior can be determined. An analytical model was proposed by Kusoglu et al. [27] to calculate the swelling pressure as a function of water (or polymer) volume fraction, using a discrete-parameter mechanics approach, based on the nanostructure of PFSA membranes.

The deformation of the polymer matrix with Young's modulus, E_{pm}, due to the growth of the water domains is characterized analytically, based on the RVEs idealizing the nanostructure of the swollen PFSA. From the compressive force generated in the polymer matrix during the growth of water domains, we can define the swelling pressure, P, as

$$P = E_{pm}\left\{\left[1+\kappa\left((1-\phi_w)^{-1/3}-1\right)\right]\left(\frac{1-\phi_{pore}^{1/n}}{1-\phi_{pore}^{dry\,1/n}}\right)\right\}\left\{1\right\}\left(\qquad (9)$$

where κ is the *non-affine swelling ratio*, a measure of the relationship between the macroscopic swelling (of the sample membrane) and the microscopic swelling (of the water domains in the nanostructure), ϕ_{pore}^{dry} is the pore (water + ion) volume fraction in the dry membrane and n is a factor depending on the geometry of the water domains. For cylindrical domains, $n = 2$ which was shown to yield good agreement with the measured sorption data [27]. The thermodynamic equilibrium for the PFSA polymer and the external water can be written as [79,80]

$$\ln\frac{a_p}{a_w} = -\frac{\overline{V}_w}{RT}P \qquad (10)$$

where a_w is the activity of the water external to the polymer (or relative humidity of the surrounding air), and a_p is the activity internal to the polymer, T is the absolute temperature, R is the universal gas constant, P is the swelling pressure applied by the

[3] This conclusion may change for compressively loaded structure depending on the fluid occupying the material voids. An investigation of compressively loaded structure is left for a future study. Furthermore, physical properties (e.g. conduction) might change due to the fluid occupying the voids, but such investigation is beyond the scope of the current paper.

polymer matrix to the water domains and $\overline{V}_w$ is the molar volume of water. The water content within the membrane consists of chemically *bound water*, λ^B, and *free water*, λ^F [10,36,80–82]. The water activity within the membrane can be approximated as the mole fraction of the free water within the membrane, i.e. $a_p = \lambda^F/(1+\lambda^F)$ [80–82]. The formulation for bound water as a function of water activity is taken from [81,82]. Consequently, the following implicit expression (from Eq.(10)) can be used to analyze the sorption behavior of PFSA membrane with the help of the pressure formulation in Eq. (9)

$$\frac{\lambda^F(\phi_w)}{1+\lambda^F(\phi_w)} = \frac{RH}{100}\exp\left[-\frac{\overline{V}_w}{RT}P(\phi_w,T)\right]. \tag{11}$$

References

[1] Mauritz KA, Moore RB. Chemical Reviews 2004;104(10):4535–85.
[2] Eikerling M, Kornyshev AA, Kucernak AR. Physics Today 2006;59(10):38–44.
[3] Mathias MF, Makharia R, Gasteiger HA, Conley JJ, Fuller TJ, Gittleman CJ, et al. Electrochemical Society Interface 2005;14(3):24–35.
[4] Rajendran RG. MRS Bulletin 2005;30(8):587–90.
[5] Beuscher U, Cleghorn SJC, Johnson WB. International Journal of Energy Research 2005;29(12):1103–12.
[6] Gebel G. Polymer 2000;41(15):5829–38.
[7] Schmidt-Rohr K, Chen Q. Nature Materials 2008;7(1):75–83.
[8] Hsu WY, Gierke TD. Journal of Membrane Science 1983;13(3):307–26.
[9] Yeo SC, Eisenberg A. Journal of Applied Polymer Science 1977;21(4):875–98.
[10] Laporta M, Pegoraro M, Zanderighi L. Physical Chemistry Chemical Physics 1999;1(19):4619–28.
[11] Gierke TD, Munn GE, Wilson FC. Journal of Polymer Science Polymer Physics Edition 1981;19(11):1687–704.
[12] Roche EJ, Pineri M, Duplessix R, Levelut AM. Journal of Polymer Science, Part B: Polymer Physics 1981;19(1):1–11.
[13] Fujimura M, Hashimoto T, Kawai H. Macromolecules 1982;15(1):136–44.
[14] Starkweather HW. Macromolecules 1982;15(2):320–3.
[15] Aldebert P, Dreyfus B, Pineri M. Macromolecules 1986;19(10):2651–3.
[16] Dreyfus B, Gebel G, Aldebert P, Pineri M, Escoubes M, Thomas M. Journal De Physique 1990;51(12):1341–54.
[17] Gebel G, Lambard J. Macromolecules 1997;30(25):7914–20.
[18] Haubold HG, Vad T, Jungbluth H, Hiller P. Electrochimica Acta 2001;46(10–11):1559–63.
[19] Gruger A, Regis A, Schmatko T, Colomban P. Vibrational Spectroscopy 2001;26(2):215–25.
[20] Weber AZ, Newman J. Journal of the Electrochemical Society 2003;150(7):1008–15.
[21] Kim MH, Glinka CJ, Grot SA, Grot WG. Macromolecules 2006;39(14):4775–87.
[22] Termonia Y. Polymer 2007;48(5):1435–40.
[23] Loppinet B, Gebel G, Williams CE. Journal of Physical Chemistry B 1997;101(10):1884–92.
[24] Rubatat L, Rollet AL, Gebel G, Diat O. Macromolecules 2002;35(10):4050–5.
[25] Gebel G, Diat O. Fuel Cells 2005;5(2):261–76.
[26] Kusoglu A, Santare MH, Karlsson AM, Cleghorn S, Johnson WB. Journal of Polymer Science, Part B: Polymer Physics 2008;46(22):2404–17.
[27] Kusoglu A, Santare MH, Karlsson AM. Polymer 2009;50(11):2481–91.
[28] Kusoglu A, Tang Y, Lugo M, Karlsson AM, Santare MH, Cleghorn S, et al. Journal of Power Sources 2010;195(2):483–92.
[29] Tang Y, Karlsson AM, Santare MH, Gilbert M, Cleghorn S, Johnson WB. Materials Science and Engineering A 2006;425(1–2):297–304.
[30] Kim S, Mench MM. Journal of Power Sources 2007;174(1):206–20.
[31] Roche EJ, Pineri M, Duplessix R. Journal of Polymer Science, Part B: Polymer Physics 1982;20(1):107–16.
[32] Cirkel PA, Okada T. Macromolecules 2000;33(13):4921–5.
[33] Morris DR, Sun XD. Journal of Applied Polymer Science 1993;50(8):1445–52.
[34] Springer TE, Zawodzinski TA, Gottesfeld S. Journal of the Electrochemical Society 1991;138(8):2334–42.
[35] Weber AZ, Newman J. Journal of the Electrochemical Society 2004;151(2):311–25.
[36] Thompson EL, Capehart TW, Fuller TJ, Jorne J. Journal of the Electrochemical Society 2006;153(12):A2351–62.
[37] Fontanella JJ, Edmondson CA, Wintersgill MC, Wu Y, Greenbaum SG. Macromolecules 1996;29(14):4944–51.
[38] Siu A, Schmeisser J, Holdcroft S. Journal of Physical Chemistry B 2006;110(12):6072–80.
[39] Okada T, Xie G, Gorseth O, Kjelstrup S, Nakamura N, Arimura T. Electrochimica Acta 1998;43(24):3741–7.
[40] Hsu WY, Gierke TD. Macromolecules 1982;15(1):101–5.
[41] Iijima M, Sasaki Y, Osada T, Miyamoto K, Nagai M. International Journal of Thermophysics 2006;27(6):1792–802.
[42] Zawodzinski TA, Derouin C, Radzinski S, Sherman RJ, Smith VT, Springer TE, et al. Journal of the Electrochemical Society 1993;140(4):1041–7.
[43] Slade S, Campbell SA, Ralph TR, Walsh FC. Journal of the Electrochemical Society 2002;149(12):A1556–64.
[44] Choi P, Jalani NH, Thampan TM, Datta R. Journal of Polymer Science, Part B: Polymer Physics 2006;44(16):2183–200.
[45] Eikerling M, Kornyshev AA, Stimming U. Journal of Physical Chemistry B 1997;101(50):10807–20.
[46] Saito M, Hayamizu K, Okada T. Journal of Physical Chemistry B 2005;109(8):3112–9.
[47] Onishi LM, Prausnitz JM, Newman J. Journal of Physical Chemistry B 2007;111(34):10166–73.
[48] Cappadonia M, Erning JW, Niaki SMS, Stimming U. Solid State Ionics 1995;77:65–9.
[49] Divisek J, Eikerling M, Mazin V, Schmitz H, Stimming U, Volfkovich YM. Journal of the Electrochemical Society 1998;145(8):2677–83.
[50] Satterfield MB, Benziger JB. Journal of Polymer Science Part B: Polymer Physics 2009;47(1):11–24.
[51] Kawano Y, Wang T, Palmer RA, Aubuchon SR. Polímeros: Ciência e Tecnologia 2002;12(2):96–101.
[52] Eisenberg A. Macromolecules 1970;3(2):147–54.
[53] Dreyfus B. Journal of Polymer Science, Part B: Polymer Physics 1983;21(11):2337–47.
[54] Liu D, Kyriakides S, Case SW, Lesko JJ, Li YX, McGrath JE. Journal of Polymer Science Part B: Polymer Physics 2006;44(10):1453–65.
[55] Solasi R, Zou Y, Huang XY, Reifsnider K. Mechanics of Time-Dependent Materials 2008;12(1):15–30.
[56] Bauer F, Denneler S, Willert-Porada M. Journal of Polymer Science, Part B: Polymer Physics 2005;43(7):786–95.
[57] Majsztrik PW, Satterfield MB, Bocarsly AB, Benziger JB. Journal of Membrane Science 2007;301(1–2):93–106.
[58] Chen Q, Schmidt-Rohr K. Macromolecular Chemistry and Physics 2007;208(19–20):2189–203.
[59] Choi P, Jalani NH, Datta R. Journal of the Electrochemical Society 2005;152(3):E123–30.
[60] Dreyfus B. Macromolecules 1985;18(2):284–92.
[61] Eisenberg A, Hird B, Moore RB. Macromolecules 1990;23(18):4098–107.
[62] Pineri M, Volino F, Escoubes M. Journal of Polymer Science, Part B: Polymer Physics 1985;23(10):2009–20.
[63] Starkweather HW, Chang JJ. Macromolecules 1982;15(3):752–6.
[64] Schlick S, Gebel G, Pineri M, Volino F. Macromolecules 1991;24(12):3517–21.
[65] Rae PJ, Brown EN. Polymer 2005;46(19):8128–40.
[66] Thampan T, Malhotra S, Tang H, Datta R. Journal of the Electrochemical Society 2000;147(9):3242–50.
[67] Gibson LJ, Ashby MF. Cellular solids: structure and properties. 2nd ed. New York: Cambridge University Press; 1997.
[68] Ashby MF. Philosophical Transactions of the Royal Society A: Mathematical Physical and Engineering Sciences 2006;364(1838):15–30.
[69] Gibson LJ. Journal of Biomechanics 2005;38(3):377–99.
[70] Jullien R, Olivi-Tran N, Hasmy A, Woignier T, Phalippou J, Bourret D, et al. Journal of Non-Crystalline Solids 1995;188(1–2):1.
[71] Woignier T, Phalippou J. Journal of Non-Crystalline Solids 1987;100(1–3):404–8.
[72] Woignier T, Phalippou J, Hdach H, Larnac G, Pernot F, Scherer GW. Journal of Non-Crystalline Solids 1992;147:672–80.
[73] Emmerling A, Fricke J. Journal of Non-Crystalline Solids 1992;145(1–3):113–20.
[74] Woignier T, Pelous J, Phalippou J, Vacher R, Courtens E. Journal of Non-Crystalline Solids 1987;95–6:1197–202.
[75] Woignier T, Despetis F, Alaoui A, Etienne P, Phalippou J. Journal of Sol-Gel Science and Technology 2000;19(1–3):163–9.
[76] Woignier T, Reynes J, Alaoui AH, Beurroies I, Phalippou J. Journal of Non-Crystalline Solids 1998;241(1):45–52.
[77] Woignier T, Phalippou J, Vacher R. Journal of Materials Research 1989;4(3):688–92.
[78] Shih WH, Shih WY, Kim SI, Liu J, Aksay IA. Physical Review A 1990;42(8):4772–9.
[79] Hiemenz PC, Lodge TP. Polymer chemistry. 2nd ed. Boca Raton: CRC Press; 2007.
[80] Mauritz KA, Rogers CE. Macromolecules 1985;18(3):483–91.
[81] Choi P, Jalani NH, Datta R. Journal of the Electrochemical Society 2005;152(3):E84–9.
[82] Choi PH, Datta R. Journal of the Electrochemical Society 2003;150(12):E601–7.